Applied Geochemistry 42 (2014) 38–44

Contents lists available at ScienceDirect

Applied Geochemistry

journal homepage: www.elsevier.com/locate/apgeochem

Transport of *Sporosarcina pasteurii* in sandstone and its significance for subsurface engineering technologies

Dominique J. Tobler [a,*], Mark O. Cuthbert [b,c], Vernon R. Phoenix [a]

[a] School of Geographical and Earth Sciences, University of Glasgow, Gregory Building, Glasgow G12 8QQ, UK
[b] Water Sciences (Hydrogeology), School of Geography, Earth and Environmental Sciences, University of Birmingham, Birmingham B15 2TT, UK
[c] Connected Waters Initiative Research Centre, The University of New South Wales, 110 King St., Manly Vale, NSW 2093, Australia

ARTICLE INFO

Article history:
Received 23 August 2013
Accepted 8 January 2014
Available online 18 January 2014
Editorial handling by B. Ngwenya

ABSTRACT

The development of microbially mediated technologies for subsurface remediation and rock engineering is steadily increasing; however, we are lacking experimental data and models to predict bacterial movement through rock matrices. Here, breakthrough curves (BTCs) were obtained to quantify the transport of the ureolytic bacterium, *Sporosarcina pasteurii*, through sandstone cores, as a function of core length (1.8–7.5 cm), bacterial density (4×10^6 to 9×10^7 cells/ml) and flow rate (5.8–17.5 m/s). *S. pasteurii* was easily immobilised within the homogeneous sandstone matrix (>80%) in comparison to a packed sand column (<20%; under similar experimental conditions), and percentage recovery decreased almost linearly with increasing rock core length. Moreover, a decrease in bacterial density or flow rate enhanced bacterial retention. A numerical model based on 1D advection dispersion models used for unconsolidated sand was fitted to the BTC data obtained here for sandstone. Good agreement between data and model was obtained at shorter rock core lengths (<4 cm), suggesting that physicochemical filtration processes are similar in homogeneous packed sand and sandstones at these lengths. Discrepancies were, however observed at longer core lengths and with varying flow rates, indicating that the attributes of consolidated rock might impact bacterial transport progressively more with increasing core length. Implications of these results on microbial mineralisation technologies currently being developed for sealing fluid paths in subsurface environment is discussed.

1. Introduction

The transport of microorganisms through porous rock media is a crucial factor for a variety of subsurface remediation and engineering technologies including *in situ* bioremediation of contaminants (e.g., Li et al., 2011), microbially enhanced oil recovery (Shabani et al., 2011) and microbially induced mineral precipitation for pore space and fracture plugging to control fluid flow (e.g., Cuthbert et al., 2013; Ferris et al., 1996; Phillips et al., 2013; Tobler et al., 2012), soil stabilization (e.g., van Paassen et al., 2010 and reference therein) and solid-phase capture of pollutants (e.g., Fujita et al., 2010; Lauchnor et al., 2013; Mitchell and Ferris, 2005). Moreover, accurate prediction of bacterial transport is valuable for risk assessment of pathogenic organisms (e.g., viruses, protozoa, or bacteria) introduced to the subsurface environment by infiltrating wastewaters (e.g., Pachepsky et al., 2006).

There is an extensive literature on the transport of bacteria in saturated packed columns (e.g., Bradford et al., 2006; Ding, 2010; Liu et al., 2011; Olson et al., 2005; Stevik et al., 2004; Stumpp et al., 2011; Torkzaban et al., 2008) where breakthrough curve analysis and in some cases magnetic resonance imaging were used to determine the impact of physical, chemical and biological parameters on bacterial retardation, dispersion and diffusion under both static and advective flow conditions. Transport of bacteria can vary considerably between different bacterial strains even when they exhibit similar cell morphologies and surface characteristics (Liu et al., 2011; Stumpp et al., 2011). This suggests that transport parameters cannot be generalised and need to be determined for each organism individually. A disadvantage of packed column experiments is that they lack the porosity, permeability, hydrodynamics and heterogeneities of consolidated rock systems: factors that have a marked impact on transport in the subsurface.

To date, there are very few studies that have investigated bacterial transport in rock. These included laboratory studies in fractured volcanic tuff and Berea sandstone (Jang et al., 1983; Story et al., 1995), and field investigations in fractured crystalline bedrock (Becker et al., 2003; Champ and Schroeter, 1988). Again, variations in transport behaviour were observed for different bacterial species, with one study also reporting substantial blocking of pore throats with an increase in injected bacterial density (Jang et al., 1983). In these studies, no model fits for the experimental

* Corresponding author. Present address: Nano-Science Center, Department of Chemistry, University of Copenhagen, 2100 Copenhagen, Denmark. Tel.: +45 35 32 02 23.
E-mail address: dominique.tobler@nano.ku.dk (D.J. Tobler).

0883-2927/$ - see front matter © 2014 Elsevier Ltd. All rights reserved.
http://dx.doi.org/10.1016/j.apgeochem.2014.01.004

breakthrough curves were presented, and thus little information on transport parameters was given. This knowledge however, is important to develop realistic models to predict bacterial transport through subsurface rock as needed for the various applications listed above. Some information could certainly be transferred from transport studies of viruses and colloids through rock, but these investigations focussed mainly on fractured rock systems both at field (e.g., McKay et al., 1997) and laboratory scale (e.g., Mondal and Sleep, 2013; Ojha et al., 2011). The hydraulic regime in fractures is very different from that associated with matrix flow and grain porosity. In fact, it is difficult to immobilise bacteria onto fracture surfaces, as has been observed in field studies on microbial mineralisation for fracture sealing (Cuthbert et al., 2013). This complicates transfer of transport parameters from fractured to porous systems.

The literature on bacterial transport through porous rock is thus limited, particularly with regards to transport modelling. Here, we determined breakthrough curves of *Sporosarcina pasteurii* in Bentheimer sandstone as a function of core length, bacterial density, and flow rate. A bacterial transport model was developed to fit the breakthrough curve data from *S. pasteurii* in Bentheimer sandstone and to infer the dominant transport processes.

We focussed on *S. pasteurii* as it is being extensively utilised in the development of technologies for pore space and fracture plugging to control fluid flow and prevent leaks in CO_2 storage reservoirs, nuclear waste repositories, or oil recovery sites. These technologies utilise the bacteria's ability to precipitate large quantities of calcite via urea hydrolysis. Pore space plugging using this process has been successful at various scales (e.g., Cuthbert et al., 2013; Ferris et al., 1996; Phillips et al., 2013; Sham et al., 2013; Tobler et al., 2012; van Paassen et al., 2010). However, a re-occurring challenge is to avoid enhanced cementation near the injection area. It is well accepted that this issue occurs because the injected bacteria do not get distributed evenly throughout the entire length of the porous system before calcite precipitation is induced. This demonstrates the need for a detailed understanding of how *S. pasteurii* is transported through porous systems. Critically, ureolysis-driven calcite precipitation is being developed for application in subsurface rock environments, thus we cannot rely on breakthrough data from unconsolidated columns and must enhance our understanding of bacterial transport in consolidated rock systems.

2. Methodology

2.1. Bacterial culturing

Transport studies were conducted with the soil-inhabiting, urease-positive bacterial strain *S. pasteurii* (ATCC 11859). *S. pasteurii* was grown at 30 °C in brain heart infusion broth supplemented with urea (20 g L^{-1}). Cells were harvested by vacuum filtration once they reached the stationary phase, i.e., all nutrients were used up and no further cell divisions occurred. *S. pasteurii* suspensions were prepared in deionised water at the desired optical density and adjusted to pH 7.5 (see details in Tobler et al., 2011). The tested bacterial densities of 0.1, 0.5 and 1.0 OD_{600} correspond to approximately 3.7×10^6, 3.3×10^7, 8.6×10^7 cells ml^{-1}, respectively (based on the *S. pasteurii* OD/cell number conversion, Ramachandran et al., 2001). Note that the OD of the injected bacterial suspensions remained constant over the course of the experiments (between 30 and 90 min) showing that no additional cell divisions occurred. Moreover, the viability of *S. pasteurii* cells was not greatly affected by their exposure to deionised water and transport through the sandstone matrix as verified by measuring similar ureolytic activity in the influent and effluent (approximately 10 mM min^{-1} OD^{-1}).

2.2. Experimental details

Experiments were conducted with Bentheimer sandstone cores (3.6 cm diameter; Kocurek Industries). Bentheimer sandstone is a fairly homogeneous rock, consisting mainly of quartz (~95%) with a small fraction of feldspars and clays (⩽5%) and trace amounts of calcite and dolomite (Maloney et al., 1990). It lacks sedimentary structures and is characterised by irregular grains and a wide grain size distribution (diameters between 80 and 600 μm, average ~190 μm), which is slightly screwed to larger grains (Dautriat et al., 2009; Maloney et al., 1990). The porosity of the sandstone was 23% and the permeability was 2.4×10^{-8} cm^2.

Rock cores were, encased in a silicon tube sleeve (3.6 cm inner diameter) with PTFE in- and outlet plugs. The silicon tubing provided a tight fit around the cores and plugs ensuring that the injected solution passed through the core and not along the sides. Prior to any experiments, air was pumped from the sandstone cores, which were then saturated and flushed with deionised water. Flow-through experiments were carried out in vertical position, with bottom to top flow. The transport of *S. pasteurii* through Bentheimer sandstone was examined as a function of varying rock core length (1.8, 3.8 and 7.5 cm), bacterial density (0.1, 0.5 and 1.0 optical density at 600 nm), and injection rate (1 and 3 ml min^{-1}, Table 1). Nitrate (0.3 mM) was used as a conservative tracer. For all experiments, 2.7 pore volumes (Table 1) of either bacterial suspension or tracer were injected and then the flow was switched to deionised water. 1 ml effluent samples were continuously collected throughout the injection process and the bacterial and tracer concentration were determined by measuring their optical density spectrophotometrically at 600 nm and 220 nm, respectively. Most experimental conditions were tested in triplicate with each replicate experiment conducted on a different day and using a fresh sandstone core. This ensured that the observed differences accounted for slight variations in rock texture and structure and confirmed reproducibility. Effluent concentration profiles over time were normalised to influent bacterial and tracer concentration, respectively and plotted versus eluted pore volume. Replica breakthrough curves were averaged and then compared with results from mathematical modelling detailed below.

2.3. Bacterial transport modelling

The transport of bacteria in porous matrices is controlled by several processes normally described using an advection

Table 1
Tested experimental conditions and % recovery of tracer and bacteria as determined from the area under the breakthrough curve.

Injected media	Core length (cm)[a]	Flow rate[b] (ml min^{-1})	# Replicas	% Recovery
0.3 mM NO_3 (Tracer)	1.8	1	3	100 ± 0.4
	3.8	1	3	100 ± 1.4
	7.5	1	3	100 ± 0.9
	7.5	3	3	100 ± 0.0
0.1 OD *S. pasteurii*	3.8	1	2	36.0 ± 8.0
	7.5	3	1	16.3
0.5 OD *S. pasteurii*	1.8	1	3	63.9 ± 17.9
	3.8	1	3	34.6 ± 11.0
	7.5	3	1	19.5
1.0 OD *S. pasteurii*	1.8	1	3	74.5 ± 9.4
	3.8	1	3	43.6 ± 13.9
	7.5	1	3	10.3 ± 5.7
	7.5	3	1	24.2

[a] Pore volumes for 1.8, 3.8 and 7.5 cm cores were 4.5, 9.4 and 18.4 cm^3, respectively.
[b] Flow rates of 1 and 3 ml min^{-1} correspond to interstitial velocities of 5.8 and 17.5 m/day.

dispersion equation (ADE) modified with mass transfer terms in account for attachment/detachment/straining of bacteria and/or decay terms due to bacterial inactivation, grazing or death (Tufenkji, 2007). For this study we used COMSOL Multiphysics (v. 4.3a) to test a variety of model structures based on existing 1-D ADE approaches for packed columns in the literature in order to test which processes needed to be included to reasonably match the observations made in a homogeneous sandstone rock. The best model formulation included an irreversible attachment process (kC) as well as a kinetic reversible attachment process (dS/dt) in the form of a Langmuir isotherm (bilinear adsorption model; Fetter, 1998) as follows:

$$\frac{\partial C}{\partial t} = D\frac{\partial^2 C}{\partial x^2} - v\frac{\partial C}{\partial x} - kC - \frac{\partial S}{\partial t} \quad (1)$$

$$\frac{\partial S}{\partial t} = K_L(K_d C(S_{\max} - S) - S) \quad (2)$$

where C is the concentration of bacteria (OD) or solute in the aqueous phase at distance x and time t, S is the concentration of reversibly attached bacteria (OD) up to a maximum of S_{max}, v is the average linear velocity (equal to the fluid flux divided by the porosity), K_d and K_l are partition and Langmuir coefficients respectively, and D is the coefficient of hydrodynamic dispersion defined as:

$$D = \alpha v + D_o \quad (3)$$

where α is the hydrodynamic dispersivity and D_0 is the coefficient for molecular diffusion or bacterial motility. The irreversible attachment coefficient k may include terms for both straining (physical filtration) and attachment (physicochemical filtration), but if the former is assumed to be insignificant (see later discussion), it may be defined using the classical colloid filtration theory (CFT) equation as:

$$k = k_{att} = \frac{3(1-\varepsilon)v\eta_0\alpha_c}{2d_c} \quad (4)$$

where α_c is the attachment efficiency, d_c is average grain size, ε is the porosity, η_0 is single collector contact efficiency (Liu et al., 2011). Despite the physical theory behind Eq. (4), not all the parameters are able to be determined *a priori* and thus k remains a model calibration parameter.

Decay terms were not included in the model as the viability and activity of the bacteria was not affected by the experimental procedure (see above). Fixed flux flow boundary conditions were used to control the advective flow velocity and the upstream transport boundary was defined using a concentration flux condition. The downstream transport boundary flux was set equal to the sum of the advective and diffusive flux components at a sufficient distance downstream to ensure the results at the column outlet distance were not sensitive to its position. The total mass flux at the distance from the upstream boundary corresponding with the length of the experimental column was output from the models for comparisons to the observed breakthrough curves.

Models were initially run using parameters for the conservative tracer to calibrate the hydrodynamic dispersivity term (α) for each column, which was left unaltered for the refinement of the bacterial transport model. D_0 was then omitted since it is negligible at the flow velocities and α values in this study. Our approach for refining the bacterial transport model was to keep parameters constant across all models to avoid 'overtuning' at the expense of losing information about the generalisation of our results with regard to process understanding. First the value of k was set to produce acceptable mass balances with regard to the bacterial mass retained in the columns by altering the value of α_c. Then, in order to fit the shapes of the breakthrough curves, the remaining unconstrained parameters (S_{max}, K_d and K_l) were varied to produce an acceptable fit across all models. It is worth noting that the sharp peaks, i.e., sudden increase in recovery followed by a quick decrease in recovery over 2–4 data points (in particular at rock core lengths of 1.8 and 3.8 cm, Figs. 1B and 2) were visually ignored during the manual refinement of the applied model. This was justified by the timing of the onset of the peaks coinciding with the short interruption in fluid flow (<5 s) during fluid changeover, which then led to a sudden increase in release of bacterial cells.

3. Results and discussion

The conservative tracer nitrate yielded 100% recovery under all tested conditions (Table 1, Fig. 1A) indicating that no tracer molecules attached to the mineral surfaces of the sandstone (consists mainly of quartz). This confirmed the assumption of elastic

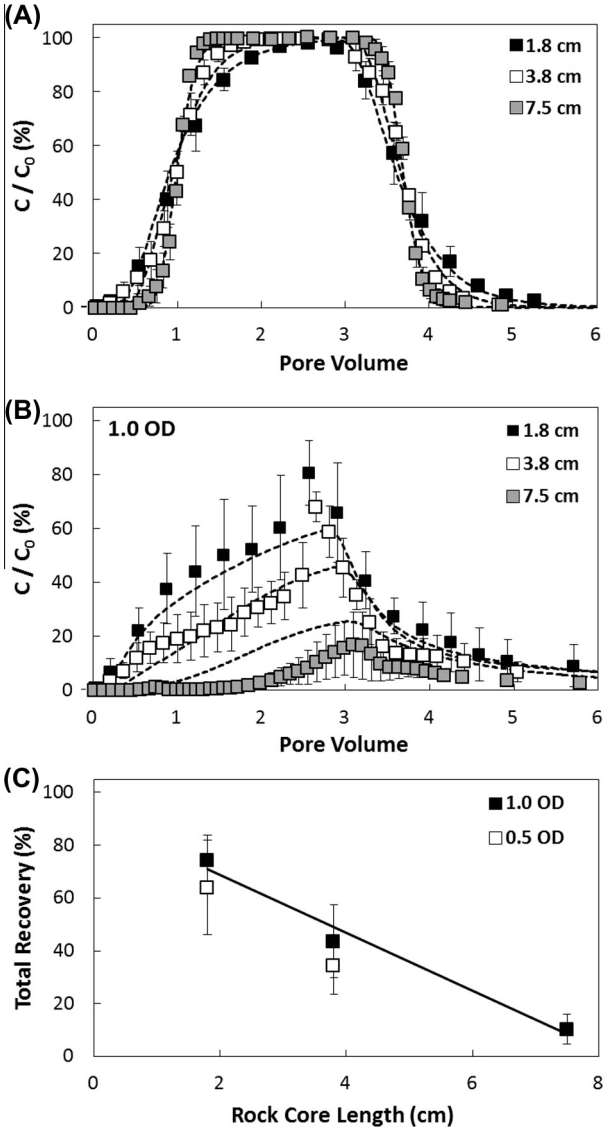

Fig. 1. Breakthrough curves of (A) the conservative tracer (0.3 mM nitrate) and (B) *S. pasteurii* (1.0 OD) as a function of rock core length (both at 1 ml min^{-1} flow rate). C/C_0 = normalised solute concentration in effluent. The dashed lines show the best fits of the mathematical transport model. (C) Total recovery of *S. pasteurii* cells (as determined from the area under the breakthrough curve) as a function of rock core length. The solid line shows an almost linear decrease (R^2 = 0.98) in % recovery with increasing core length for *S. pasteurii* at 1.0 OD. All data points represent the average of triplicate experiments with associated standard deviation (σ = 1, shown as error bars).

collisions between nitrate molecules and sandstone grains (i.e., $k = 0$). Initial modelling of the tracer experiments provided an estimate of the hydrodynamic dispersivity, $\alpha = 0.75$ cm, and this value was then used for modelling of bacterial BTCs (Table 2).

Bacterial breakthrough curves exhibited considerably lower recovery values compared to the tracer experiments, ranging from 10% to 75% (Table 1). This indicated that *S. pasteurii* cells became trapped within the sandstone. This effect was included in the numerical model using a first order rate equation for irreversible attachment (the term kC in Eq. (1)), and this proved effective in simulating the observed range of retention for the input concentrations and flow rates tested. This term alone, while effective at simulating retention quantity, poorly mimicked the shape of the bacterial breakthrough curves (data not shown). Subsequent modelling indicated that a reversible loss term with the applied Langmuir isotherm was needed to fit the shape of the breakthrough curves adequately (Figs. 1b and 2).

3.1. BTCs as a function of core length

Total bacterial cell recovery decreased almost linearly with increasing core length (Fig. 1B and C). This shows that the rate at which bacteria are immobilized within the rock matrix (i.e., % cells per cm core length) was very similar for the three different core lengths. This trend further indicates that if a 1.0 OD *S. pasteurii* suspension is injected into a Bentheimer sandstone core with length > 8 cm (under the conditions tested here), all the injected bacteria would be distributed over the first 8 cm (where the trendline intercepts the *x*-axis, Fig. 1C) and none immobilised in the remaining section of the core. Two mechanisms are most likely to be causing this effect – straining (physical filtration) and attachment (physicochemical filtration; Tufenkji, 2007). If straining was a significant mechanism, this effect should be more pronounced in the first part of the rock core and reduce with distance, potentially leading to hyper-exponential retention profiles as observed previously in unconsolidated column studies (Kasel et al., 2013 and references therein). Although the bacterial distribution along the core seems fairly homogeneous, slightly more bacteria were trapped within the 0–3.8 cm section (~54%) compared to the 3.8–7.5 cm section (~40%, Fig. 1C). Older studies have relied on geometric consideration to elucidate the presence of straining, where straining was considered likely to occur if the bacterial cell diameter is >5% of the average grain size of the medium (Ginn et al., 2002). In this study, the ratio of the *S. pasteurii* cell (average 2.8 μm in size) to average quartz grain diameter (190 μm) has a

Table 2
Transport parameters as determined by 1-D modelling for sandstone.

	Tracer	*S. pasteurii*
Estimated or measured values		
Velocity, v (m/d)	5.8/17.5[a]	5.8/17.5[a]
Porosity, ε	0.23	0.23
Average grain diameter, d_c (m)[b]	1.9×10^{-4}	1.9×10^{-4}
Dry bulk density, ρ (kg/m^3)	2104	2104
Fitted or calculated from fitted values		
Hydrodynamic dispersion, D (m^2/d)	0.04/0.13[a]	0.04/0.13[a]
Hydrodynamic dispersivity, α (m)	7.5×10^{-3}	7.5×10^{-3}
Distribution Coefficient, K_d (/OD)	–	5
Langmuir rate constant, K_l (/d)	–	100
Maximum attachment concentration, S_{max} (OD)	–	1
Collision efficiency, α_c	–	0.3
CFT attachment rate coefficient, k_{att} (/d)	–	106.1/318.6[a]
Single collector contact efficiency, η_0[c]	–	0.01

[a] Parameters for flow rates of 1 ml min^{-1} and 3 ml min^{-1}, respectively.
[b] Taken from Maloney et al. (1990) and verified by Scanning Electron Microscopy.
[c] Calculated using Eq. (4).

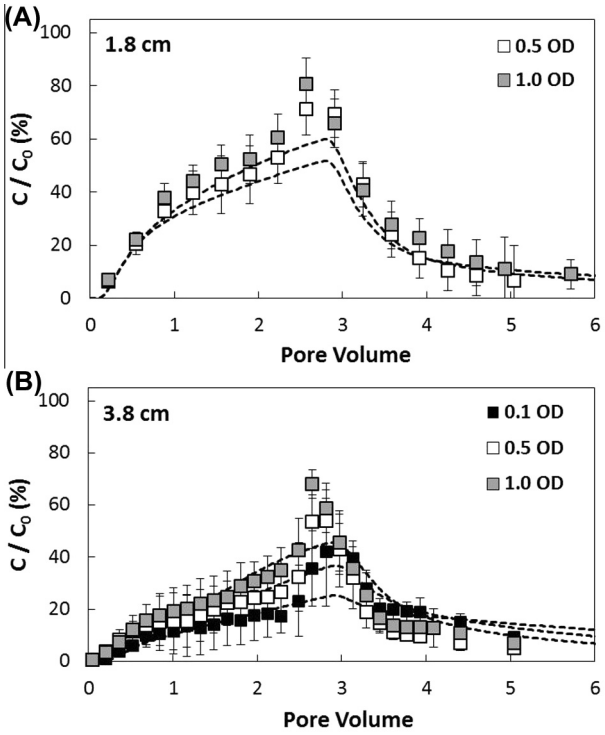

Fig. 2. Breakthrough curves of *S. pasteurii* suspensions with varying cell densities in a (A) 1.8 cm and (B) 3.8 cm sandstone core. The dashed lines show the best fits of the transport model. Each data set (except 0.1 OD) represents the average of triplicate experiments with associated standard deviation ($\sigma = 1$, shown as error bars).

value of 1.5%, which suggests that straining should not be important here. However, we also note that unconsolidated sand studies (e.g., Tufenkji, 2007 and references therein) have shown that straining is also observed at ratios ⩽1.5% and that this is caused by irregular grain shapes. The sandstone used here exhibits irregular grains and a wide distribution in grain size, pore space and pore throats (Dautriat et al., 2009; Maloney et al., 1990), suggesting that some straining likely occurred.

If straining played a minor role then the effect of enhanced retention with increasing core length should be due to physicochemical filtration (attachment), i.e., an increase in contact time between bacterial cells and mineral surfaces with increasing core length. The numerical model accounts for this via Eq. (4) and simulates the data well, as shown by R^2 (coefficient of determination) values of 0.89 for 1.8 cm and 0.80 for 3.8 cm (Fig. 1b). The only exception is the model fit for the 7.5 cm core experiment (at 1 ml min^{-1}, $R^2 = -1.65$) where bacterial retention is underestimated (Fig. 1B, dashed line, grey squares). The relatively high filtration for the longer consolidated cores could thus not be accurately described with the set of model parameters, which achieved good fits at shorter lengths. The slight discrepancy between the 7.5 cm data and model may not be surprising as there is possibly some straining taking place (a process not explicitly accounted for in the model) which leads to slightly higher retention. Moreover, the presence of other minerals (~5% of clays, feldspars, and trace amounts of calcite and dolomite) and their different surface properties may further aid bacterial immobilisation. Thus overall, the attributes of consolidated (sandstone) versus unconsolidated (sand) porous media might explain the observed discrepancies with scale.

3.2. BTCs as a function of bacterial density (OD)

S. pasteurii recovery at 1.0 OD appeared to be higher than at 0.5 OD for both 1.8 cm and 3.8 cm core experiments (Figs. 1C and 2,

Table 1). This increase in recovery with increasing cell density was further observed at higher flow rates (17.5 m/d) in 7.5 cm cores (16.3, 19.5 and 24.2 at 0.1, 0.5 and 1.0 OD respectively; Table 1). We hypothesise that the attachment coefficients are identical between experiments with varying bacterial densities (Table 2) and the observed trend is caused by the number of attachment sites being limited; these get saturated at higher bacterial densities, thus more bacteria are eluted and recovered. The success of the Langmuir form of Eq. (2) in simulating the shape of the breakthrough curves (Fig. 2) is consistent with this hypothesis. In the literature, this trend has been described as 'blocking' and has been observed in several unconsolidated sand studies (e.g., Tan et al., 1994; Camesano et al., 1999 and reference therein). For example, Tan et al. (1994) obtained identical attachment coefficients for bacterial BTCs for *Pseudomonas* with varying bacterial densities, and at similar flow rates as tested here. Similarly, they explained that at higher cell concentrations, finite retention sites would be saturated much earlier which then led to enhanced bacterial breakthrough. This further corroborates the occurrence of blocking in our experiments.

Overall, the numerical model provided good fits to the 1.8 and 3.8 cm core data as a function of different bacterial densities (R^2 values ranging from 0.66 to 0.89, Fig. 2). This showed that transport of *S. pasteurii* (as measured by OD) in short homogeneous sandstone cores follows similar laws as in unconsolidated sand columns (i.e., CFT theory combined with blocking).

3.3. BTCs as a function of flow rate

An increase in *S. pasteurii* recovery was observed with an increase in flow rate from 1 to 3 ml min^{-1} (5.8 and 17.5 m/d, respectively) in 1.0 OD experiment as shown in Fig. 3 and Table 1. This trend is in agreement with colloid filtration theory and has been observed repeatedly in packed column studies (Ding, 2010; Ginn et al., 2002; Hendry et al., 1999). It is explained by a decrease in number of collisions with increasing bulk fluid velocity (i.e., convection becomes the dominant transport process). As a result, bacterial contact with grain surfaces decreases and thus the possibility for adsorption and bacterial retention reduces. While a difference in breakthrough was observed experimentally, the model failed to simulate this difference (Fig. 3). This shows that the applied model is not very sensitive to variations in flow velocity and thus suggests the simple relationship between CFT irreversible attachment and fluid velocity (Eqs. (1) and (4)) is not entirely adequate to simulate the experimental results in this regard for the sandstone tested here. Indeed, the presence of some straining could partly explain this discrepancy. Straining is predicted to increase with decreasing flow rates (Cushing and Lawler, 1998), and this has also been shown in bacterial transport studies in unconsolidated material (e.g., Bradford et al., 2006). Thus, we speculate that the larger difference in bacterial recovery observed in the experimental data is likely due to straining having a higher impact at the lower flow velocity (5.8 m/d), while at 17.5 m/d straining is less noticeable, and hence we observe a better agreement between the data and model at v = 17.5 m/d (Fig. 3). As discussed above, we also envisage that the presence of some minerals other than quartz (with different surface properties) affect bacterial transport behaviour, an aspect that is difficult to include in models, without constraint from further laboratory data.

It is important to note that at lower flow rates, diffusion and dispersion as a result of bacterial mobility can considerably affect bacterial breakthrough (in comparison to non-motile bacteria). Studies of bacterial transport in sand columns indicate that as pore velocity decreases, recovery of non-motile strains decreases, while recovery of motile strains increases or remains the same (e.g., Camesano and Logan, 1998; Liu et al., 2011). The bacterium *S. pasteurii* studied here is motile (Vos et al., 2009). However, we observed lower % recovery with decreasing velocity as would be expected for non-motile strains. We thus hypothesise that for this particular motile strain, bacterial diffusion and dispersion played a negligible role at the flow velocities (5.5 and 17.5 m/d) and experimental conditions tested here.

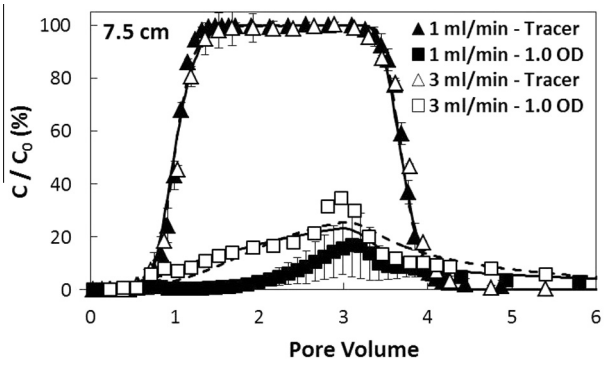

Fig. 3. Breakthrough curves of tracer (0.3 mM nitrate) and *S. pasteurii* (at 1.0 OD) as a function of flow rate in a 7.5 cm sandstone core. The solid and dashed lines show the best fits of the transport model to the 1 ml min^{-1} data (triplicate experiments) and 3 ml min^{-1} data (single experiments), respectively.

3.4. Comparison between consolidated and unconsolidated material

This study aimed to enhance our limited understanding of bacterial transport in consolidated rock by providing experimental breakthrough data combined with numerical modelling. Results showed that bacterial trapping in homogeneous sandstone is similar to transport through unconsolidated sand, however, there are discrepancies that are difficult to explain with existing models for unconsolidated sand.

At velocities of 5.8–17.5 m/d, rates that are comparable to those used for subsurface field injections (e.g., oil recovery, pump and treat approach), less than 20% of the biomass was recovered at the end of a 7.5 cm long sandstone core. In sand columns, with equivalent dimensions and at identical flow rates, a recovery greater than 80% is observed (e.g., Liu et al., 2011). Indeed, sandstone exhibits a considerably lower porosity (23%) and a lower permeability (2.4×10^{-8} cm^2) compared to a packed column (38% and 4.5×10^{-8} cm^2, respectively), and this certainly explains some of the observed differences in recovered biomass. The applied numerical model, which is based on 1D ADE models successfully used for unconsolidated sand, shows very good agreement for the short rock core experiments (i.e., 1.8 and 3.8 cm, Figs. 1B and 2). At longer distances (i.e., 7.5 cm) and under different flow rates, the agreement between data and model is however, less satisfactory, suggesting a 'break down' of the applied model. It is difficult to pinpoint the parameters responsible for this divergence, particularly in the absence of many other studies that quantified and modelled bacterial breakthrough in rock matrices. Possibly, attributes of this consolidated rock including a wider grain size distribution, smaller pore spaces and throats, along with higher abundance of dead-end pores (due to cementation) and irregular grains have contributed to some straining taking place. Moreover, the presence of other minerals will have certainly affected physicochemical filtration. The relationships between pore velocity and attachment in consolidated natural samples is thus not as simple as in unconsolidated, pure systems.

It is important to reiterate that Bentheimer sandstone is a fairly homogeneous rock, consisting mainly of quartz (95%) with a small fraction of feldspars and clay (≤5%) and lacking sedimentary structures (Maloney et al., 1990). Many other natural porous rocks

exhibit a smaller porosity and permeability, smaller pore throats, and in many cases they are also more heterogeneous in texture and mineralogy. Thus, to improve current transport models to allow prediction of bacteria injected into subsurface rock environments, as required for several subsurface technologies, more work needs to be focussed on characterisation and understanding bacterial transport through rock matrices. More BTC studies will increase understanding of bulk processes, but new approaches and techniques will also need to be developed to provide spatially resolved data to allow correlation of small-scale variations in rock structure and texture to bacterial attachment behaviour.

3.5. Implication for ureolysis-driven calcite precipitation

This study shows that *S. pasteurii* cells are easily trapped in sandstone (3.6 cm diameter, 1.8–7.5 cm length), even at relatively high velocities, i.e., 6.2 m/d. It is shown here and in previous studies that bacterial transport can be enhanced if injection rates and thus interstitial flow velocities are increased. Moreover, once mineral surfaces within a rock specimen are saturated with bacterial cells (as implied by the Langmuir kinetic model), an increase in bacterial breakthrough may be expected. It is, however, likely that continued bacterial injection will eventually lead to clogging of pore throats, and reduction of permeability, an aspect that should be investigated in future studies.

An interesting observation is that although slightly more bacteria were trapped within the first few cm (~54% in 0–3.8 cm section compared to ~40% in 3.8–7.5 cm section), bacterial distribution along the core was fairly homogeneous (Fig. 1C). With regards to the use of bacteria to induce mineral precipitation for pore space filling, we can thus assume that cells get relatively evenly distributed along the rock core during the initial bacterial injection (under the tested conditions). This even distribution of cells would, at least in the first instance, be advantageous as it would help to ensure a more even spread porosity reduction. It is therefore important to understand what happens thereafter. In most cases, a solution of $CaCl_2$ and urea is injected to induce calcite precipitation. This will lead to the formation of new mineral surfaces within pore spaces (Cuthbert et al., 2012). Critically, this will change the size and distribution of pore spaces and pore throats within the rock, surface reactivity and flow dynamics. Furthermore, the presence of new calcite surfaces is more favourable for *S. pasteurii* trapping (in comparison to quartz, Tobler et al., 2012). If more bacteria are then injected into this modified matrix (as would be required to continue pore space filling and sealing), we can assume that bacterial distribution and % recovery will be substantially different compared to the initial injection. To what degree, however, is difficult to predict, as to date there is little other data on transport in consolidated material available. Thus, further investigations are needed to advance process understanding in rock, and to help improve implementation strategies for microbially mediated subsurface technologies being developed worldwide.

Acknowledgements

This work was funded by an Engineering and Physical Sciences Research Council (EPSRC) Grant (EP/G063699/1). MOC was latterly supported by funding from the European Community's Seventh Framework Programme [FP7/2007–2013] under Grant Agreement No. 299091.

References

Becker, M.W., Metge, D.W., Collins, S.A., Shapiro, A.M., Harvey, R.W., 2003. Bacterial transport experiments in fractured crystalline bedrock. Ground Water 41 (5), 682–689.

Bradford, S.A., Simunek, J., Walker, S.L., 2006. Transport and straining of *E. coli* O157:H7 in saturated porous media. Water Resour. Res. 42, W12S12.

Camesano, T.A., Logan, B.E., 1998. Influence of fluid velocity and cell concentration on the transport of motile and nonmotile bacteria in porous media. Environ. Sci. Technol. 32, 1699–1708.

Camesano, T.A., Unice, K.M., Logan, B.E., 1999. Blocking and ripening of colloids in porous media and their implications for bacterial transport. Colloids Surf. A 160, 291–308.

Champ, D.R., Schroeter, J., 1988. Bacterial transport in fractured rock – a field scale tracer test at the chalk river nuclear laboratories. Water Sci. Technol. 20, 81–87.

Cushing, R.S., Lawler, D.F., 1998. Depth filtration: fundamental investigation through three-dimensional trajectory analysis. Environ. Sci. Technol. 32, 3793–3801.

Cuthbert, M.O., Riley, M.S., Handley-Sidhu, S., Renshaw, J.C., Tobler, D.J., Phoenix, V.R., Mackay, R., 2012. Controls on the rate of ureolysis and the morphology of carbonate precipitated by *S. pasteurii* biofilms and limits due to bacterial encapsulation. Ecol. Eng. 41, 32–40.

Cuthbert, M.O., Riley, M.S., McMillan, L., Handley-Sidhu, S., Tobler, D.J., Phoenix, V.R., 2013. A field and modelling study of fractured rock permeability reduction using microbially induced calcite precipitation. Environ. Sci. Technol. 47, 13637–13643.

Dautriat, J., Gland, N., Guelard, J., Dimanov, A., Raphanel, J.L., 2009. Axial and radial permeability evolutions of compressed sandstones: end effects and shear-band induced permeability anisotropy. Pure Appl. Geophys. 166, 1037–1061.

Ding, D., 2010. Transport of bacteria in aquifer sediment: experiments and modeling. Hydrogeol. J. 18 (3), 669–679.

Ferris, F.G., Stehmeier, L.G., Kantzas, A., Mourits, F.M., 1996. Bacteriogenic mineral plugging. J. Can. Petrol. Technol. 13 (8), 57–67.

Fetter, C.W., 1998. Contaminant Hydrogeology. Prentice-Hall Publishing Company, Upper Saddle River, NJ, 500 p.

Fujita, Y., Taylor, J.L., Wendt, L.M., Reed, D.W., Smith, R.W., 2010. Evaluating the potential of native ureolytic microbes to remediate a 90Sr contaminated environment. Environ. Sci. Technol. 44, 7652–7658.

Ginn, T.R., Wood, B.D., Nelson, K.E., Scheibe, T.D., Murphyc, E.M., Clement, T.P., 2002. Processes in microbial transport in the natural subsurface. Adv. Water Resour. 25, 1017–1042.

Hendry, M.J., Lawrence, J.R., Maloszewski, P., 1999. Effects of velocity on the transport of two bacteria through saturated sand. Ground Water 37, 103–112.

Jang, L.-K., Chang, P.W., Findley, J.E., Teh, F.Y., 1983. Selection of bacteria with favorable transport properties through porous rock for the application of microbial-enhanced oil recovery. Appl. Environ. Microbiol. 46 (5), 1066–1072.

Kasel, D., Bradford, S.A., Šimůnek, J., Heggen, M., Vereecken, H., Klumpp, E., 2013. Transport and retention of multi-walled carbon nanotubes in saturated porous media: effects of input concentration and grain size. Water Res. 47 (2), 933–944.

Lauchnor, E., Schultz, L., Bugni, S., Mitchell, A.C., Cunningham, A., Gerlach, R., 2013. Bacterially induced calcium carbonate precipitation and strontium co-precipitation in a porous media flow system. Environ. Sci. Technol. 47, 1557–1564.

Li, M., Mahmudov, R., Huang, C.P., 2011. Hazardous waste treatment technologies. Water Environ. Res. 83 (10), 1598–1632.

Liu, J., Ford, R.M., Smith, J.A., 2011. Idling time of motile bacteria contributes to retardation and dispersion in sand porous medium. Environ. Sci. Technol. 45 (9), 3945–3951.

Maloney, D.R., Honarpour, M.M., Brinkmeyer, A.D., 1990. The Effects of Rock Characteristics on Relative Permeability. Department of Energy Report NIPER 441, Bartlesville, OK, National Institute for Petroleum and Energy Research.

McKay, L.D., Gillham, R.W., Cherr, J.A., 1997. Field experiments in a fractured clay till: 2. Solute and colloid transport. Water Resour. Res. 29, 3879–3890.

Mitchell, A.C., Ferris, F.G., 2005. The coprecipitation of Sr into calcite precipitates induced by bacterial ureolysis in artificial groundwater: temperature and kinetic dependence. Geochim. Cosmochim. Acta 69 (17), 4199–4210.

Mondal, P.K., Sleep, B.E., 2013. Virus and virus-sized microsphere transport in a dolomite rock fracture. Water Resour. Res. 49 (2), 808–824.

Ojha, C., Surampalli, R., Sharma, P., Joshi, N., 2011. Breakthrough curves and simulation of virus transport through fractured porous media. J. Environ. Eng. 137 (8), 731–739.

Olson, M.S., Ford, R.M., Smith, J.A., Fernandez, E.J., 2005. Analysis of column tortuosity for $MnCl_2$ and bacterial diffusion using magnetic resonance imaging. Environ. Sci. Technol. 39 (1), 149–154.

Pachepsky, Y.A., Sadeghi, A.M., Bradford, S.A., Shelton, D.R., Guber, A.K., Dao, T., 2006. Transport and fate of manure-borne pathogens: modeling perspective. Agric. Water Manage. 86 (1–2), 81–92.

Phillips, A.J., Lauchnor, E., Eldring, J., Esposito, J., Mitchell, A.C., Gerlach, R., Cunningham, A.B., Spangler, L.H., 2013. Potential CO_2 leakage reduction through biofilm-induced calcium carbonate precipitation. Environ. Sci. Technol. 47, 142–149.

Ramachandran, S.K., Ramakrishnan, V., Bang, S.S., 2001. Remediation of concrete using micro-organisms. ACI Mater. J. 98 (1), 3–9.

Shabani, A.M., Alipour, S., Torsater, O., 2011. Fundamental study of pore scale mechanisms in microbial improved oil recovery processes. Transport Porous Med. 90 (3), 949–964.

Sham, E., Mantle, M.D., Mitchell, J., Tobler, D.J., Phoenix, V.R., Johns, M.L., 2013. Monitoring bacterially induced calcite precipitation in porous media using magnetic resonance imaging and flow measurements. J. Contam. Hydrol. 152, 35–43.

Stevik, T.K., Ausland, G., Hanssen, J.F., 2004. Retention and removal of pathogenic bacteria in wastewater. Water Res. 38 (6), 1355–1367.
Story, S.P., Amy, P.S., Bishop, C.W., Colwell, F.S., 1995. Bacterial transport in volcanic tuff cores under saturated flow conditions. Geomicrobiol. J. 13 (4), 249–264.
Stumpp, C., Lawrence, J.R., Hendry, M.J., Maloszewski, P., 2011. Transport and bacterial interactions of three bacterial strains in saturated column experiments. Environ. Sci. Technol. 45 (6), 2116–2123.
Tan, Y., Gannon, J., Baveye, P., Alexander, M., 1994. Transport of bacteria in an aquifer sand: experiments and model simulations. Water Resour. Res. 30, 3243–3252.
Tobler, D.J., Cuthbert, M.O., Greswell, R.B., Riley, M.S., Renshaw, J.C., Handley-Sidhu, S., Phoenix, V.R., 2011. Comparison of rates of ureolysis between *Sporosarcina pasteurii* and an indigenous groundwater community under conditions required to precipitate large volumes of calcite. Geochim. Cosmochim. Acta 75 (11), 3290–3301.
Tobler, D.J., Maclachlan, E., Phoenix, V.R., 2012. Microbially mediated plugging of porous media and the impact of differing injection strategies. Ecol. Eng. 42 (1), 270–278.
Torkzaban, S., Tazehkand, S.S., Walker, S.L., Bradford, S.A., 2008. Transport and fate of bacteria in porous media: coupled effects of chemical conditions and pore space geometry. Water Resour. Res. 44 (4), W04403.
Tufenkji, N., 2007. Modeling microbial transport in porous media: traditional approaches and recent developments. Adv. Water Resour. 30, 1455–1469.
Van Paassen, L.A., Ghose, R., van der Linden, T.J.M., van der Star, W.R.L., van Loosdrecht, M.C.M., 2010. Quantifying biomediated ground improvement by ureolysis: large-scale biogrout experiment. J. Geotech. Geoenviron. Eng. 136 (12), 1721–1728.
Vos, P., Garrity, G., Jones, D., Krieg, N.R., Ludwig, W., Rainey, F.A., Schleifer, K.H., Whitman, W.B., 2009. Bergey's Manual of Systematic Bacteriology, vol. 3, second ed. Springer-Verlag, New York, p. 518.